OncoTargets and Therapy

Dovepress
open access to scientific and medical research

Open Access Full Text Article

ORIGINAL RESEARCH

Stichoposide C Exerts Anticancer Effects on Ovarian Cancer by Inducing Autophagy via Inhibiting AKT/mTOR Pathway

Fangfang Liu[1,*]
Lumin Tang[2,*]
Mengyu Tao[3,*]
Chuang Cui[1]
Di He[2]
Longxia Li[2]
Yahui Liao[4]
Yamin Gao[5]
Jing He[5]
Fan Sun[6]
Houwen Lin[6]
He Li[1,2]

[1]Shanghai University of Traditional Chinese Medicine, Shanghai, People's Republic of China; [2]Traditional Chinese Medicine Department, Renji Hospital, School of Medicine, Shanghai Jiao Tong University, Shanghai, 200127, People's Republic of China; [3]Department of Gynecology and Obstetrics, Shanghai Key Laboratory of Gynecology Oncology, Renji Hospital, School of Medicine, Shanghai Jiao Tong University, Shanghai, 200127, People's Republic of China; [4]Shanghai Ocean University, Shanghai, People's Republic of China; [5]Shenyang Pharmaceutical University, Benxi, People's Republic of China; [6]Research Center for Marine Drugs, State Key Laboratory of Oncogenes and Related Genes, Department of Pharmacy, RenJi Hospital, School of Medicine, Shanghai JiaoTong University, Shanghai, People's Republic of China

*These authors contributed equally to this work

Correspondence: He Li; Fan Sun
Tel +86 21 51322222; +86 21 68383339
Email lihe1972@hotmail.com; sunfan2017@163.com

Purpose: Stichoposide C (STC) is a triterpene glycoside isolated from *Thelenota ananas*, which is previously demonstrated to wide spectrum of anticancer effects against various tumor cells. However, the antitumor effects and underlying molecular mechanisms in ovarian cancer (OC) cells are not fully understood. Here, we examined if and through which mechanisms STC exerts anticancer effects on OC.

Methods: CCK-8 and colony formation assays were used to detect cell viability and proliferation. Flow cytometry was used to detect apoptosis and cell cycle arrest. Protein expression and phosphorylation were measured by Western blotting analysis. Confocal fluorescence microscopy was used to observe the autophagy flux. Autophagosome formation was observed via transmission electron microscopy. Antitumor effect of STC was investigated in patient-derived organoids (PDOs) and A2780 subcutaneous xenograft tumors.

Results: STC was found that not only exerted antiproliferation activity and apoptosis but also induced autophagy. Mechanistically, STC induced autophagy via inhibited the AKT/mTOR signaling pathway in ovarian cancer cells. In addition, STC and an autophagy inhibitor 3-methyladenine (3-MA) combination treatment showed significant synergetic effects on inhibiting proliferation and promoting apoptosis in vitro. Consistent with cell experiments, STC also inhibited the growth of two OC PDOs. Finally, STC markedly reduced the growth of A2780 subcutaneous xenograft tumors without organ toxicity and activated autophagy in vivo.

Conclusion: Stichoposide C exerts in vitro and in vivo anticancer effects on ovarian cancer by inducing autophagy via inhibiting AKT/mTOR pathway. The findings warrant further prove for STC as a potential therapeutic agent for ovarian cancer.

Keywords: ovarian cancer, stichoposide C, autophagy, apoptosis, AKT/mTOR

Introduction

Ovarian cancer (OC) is the most common malignant gynecological cancer and the second cause of gynecologic cancer death in women around the world.[1,2] Although treatment for ovarian cancer, including diagnostic techniques, surgery protocols and treatment strategies, has significantly improved, the 5 years after diagnosis overall survival rate of patients remains at only 40%.[3,4] Drug resistance and recurrence remain the major problems in the treatment of ovarian cancer.[5] Therefore, novel agents and effective therapies are urgent to develop for treatment of ovarian cancer.

Sea cucumbers, which contain a wide range of bioactive compounds, have been used as food and traditional Chinese medicine.[6,7] Marine triterpene glycosides have

Received: 22 September 2021
Accepted: 20 December 2021
Published: 21 January 2022

been found in several species of sea cucumbers and some sponges, which have been found to exhibit many biologic activities such as antitumor, anti-inflammatory, antifungal and anticoagulant.[8–12] Stichoposide C (STC) is a triterpene glycoside isolated from sea cucumber Thelenota ananas, which has been reported to induce apoptosis by producing ceramides in leukemia and colorectal cancer cells.[13] Although the antitumor activity of STC has been suggested, the detailed underlying mechanisms is still unknown.

The AKT/mTOR signaling pathway plays a vital role in the regulation of cancer cells proliferation, apoptosis, multidrug resistance and metabolism, which is a poor prognostic factor for many types of cancers.[14–17] Compared to other signaling pathways, AKT/mTOR signaling pathway is one of the most frequently activated signaling pathway in human cancer, including ovarian cancer.[18–21] In addition, AKT/mTOR signaling pathway is suggested to be a key regulatory signal for autophagy, which plays an extremely important role in tumor suppression.[22,23] Therefore, autophagy-dependent cell death regulated by AKT/mTOR signaling pathway provides molecular mechanisms and implications for therapeutic intervention in ovarian cancer therapy.

In this study, we demonstrated the inhibitory effects of STC on ovarian cancer in vitro and in vivo. In addition, our results indicated that STC induced apoptosis and promoted autophagy in two ovarian cancer cell lines A2780 and SKOV3. Mechanistically, the apoptosis and autophagy induced by STC in ovarian cancer was via the inactivation of AKT/mTOR pathway.

Materials and Methods

Samples and Reagents

The samples of the sea cucumber Thelenota anax were collected at the Woody Island, Xisha, South China Sea. The specimens were stored in the Research Center for Marine Drugs, State Key Laboratory of Oncogenes and Related Genes, Renji Hospital, School of Medical, Shanghai Jiao Tong University. STC was isolated and extracted from sea cucumber *Thelenota anax* by Chuang, C (Shanghai University of Traditional Chinese Medicine, Shanghai, China) and referred to the protocol published by Yun et al.[13] The chemical structure of STC is shown in Figure S1. The purity of the STC was 95.6% determined by HPLC (Figure S2). For experiments, STC was dissolved in dimethyl sulfoxide (DMSO).

Other reagent sources are listed as follows: Cell Counting Kit-8 (CK04–50000T, Dojindo, Japan), Annexin V-FITC/ PI kit (AD10-50T, Dojindo, Japan), cisplatin (S1166, Selleck, USA), dimethylsulfoxide (DMSO, 1129E033, Solarbio, China), foetal bovine serum (FBS, 10,099, Gibco), trypsin-EDTA solution (25,200,072, Gibco), Dulbecco's Modified Eagle medium (DMEM, 11054001, Gibco), GFP-mRFP-LC3 adenoviral vectors (HB-AP2100001, HanBio Technology, Shanghai, China), 3-methyladenine (3-MA, HY-19312, MCE, USA), MK2206 (S1078, Selleck, USA), rapamycin (S1039, Selleck, USA), 2.5% glutaraldehyde fixation (DF0156, leagene Biological, Beijing, China) and bicinchoninic acid (BCA) protein assay kit (Beyotime Institute of Biotechnology, China).

Cell Lines and Cell Culture

A2780 human ovarian cancer cell lines were donated by the Shanghai Key Laboratory of Gynecologic Oncology. SKOV3 human ovarian cancer cell lines were purchased from the National Collection of Authenticated Cell Cultures (Shanghai, China). The use of the human ovarian cancer cell lines (A2780 and SKOV3) was approved by Shanghai Jiao Tong University School of Medicine, Renji Hospital Ethics Committee. Before experiments, both cell lines have been authenticated by comparing their STR profiles with the ATCC database and they have been also certified mycoplasma-free by a MycoAlert test. The cells were incubated in DMEM with 10% fetal bovine serum and maintained at 37°C in an incubator set to 5% CO_2.

CCK-8 Assay

According to the reagent instructions, cell viability was analyzed using Cell Counting Kit-8. The cells were cultured in 96-well plates at a density of 5×10^3 cells per well for 24 hours, treated with different concentrations of STC for another 24 hours or 48 hours and incubated with 100 μL of DMEM and 10 μL of CCK-8 solution at 37°C for approximately 2 hours. A multifunctional enzyme marker (Molecular Devices, USA) was used to read the absorbance of each well at 450 nm. Data analyses were performed using the GraphPad Prism software version 9.0 to calculate IC50 (Table 1).

Colony Formation Assay

A2780 and SKOV3 cells were inoculated into 6-well plates at a density of 1×10^3 cells/well. After 24 hours, the cells were treated with different concentrations of STC and

Table 1 IC50 of STC in A2780 and SKOV3 Cells at 24h and 48h

IC50 of STC in A2780 and SKOV3 cells at 24h and 48h (μM)		
	24h	48h
A2780	2.562 ± 0.03	1.443 ± 0.05
SKOV3	1.573 ± 0.06	0.832 ± 0.05

cultured at 37°C in a 5% CO_2 incubator. The medium was changed every 3 days. Colonies were allowed to form for 2 weeks. Finally, the plates were washed twice with PBS at room temperature, and the cells were fixed with 4% polyformaldehyde. Then, the cells were stained with 1% crystalline violet at room temperature for 30 minutes. All experiments were repeated three times. Image J software was used to quantify the number of colonies in three independent experiments. The colony formation rate = colony formation number/the number in controls ×100%.

Flow Cytometry Assay

A2780 and SKOV3 cells were inoculated into 6-well plates at 4×10^5 cells/well, cultured overnight and treated with different concentrations of STC. Forty-eight hours after processing, trypsin was used to collect the cells, and the cells were washed with phosphate-buffered saline. Then, according to the instructions of the reagents, cell staining was performed for 15–30 minutes using 4 μL of staining solution from an Annexin V-FITC/PI kit. Finally, the samples were analyzed via Attune™ Nxt Acoustic Focusing Flow Cytometer system (BD Biosciences, USA).

Autophagy Analysis

To detect autophagosomes and autolysosomes, A2780 and SKOV3 cells were inoculated in confocal petri dishes at 1×10^5 cells/well and cultured overnight. Then, the cells were transduced with GFP-mRFP-LC3 adenoviral vectors. After 24 hours of exposure to adenovirus, the A2780 and SKOV3 cells were treated with STC and/or autophagy inhibitors. After 24 hours, the cells were mounted on slides, and autophagic flux observation was performed with a Zeiss LSM710 confocal microscope.

Transmission Electron Microscopy

Cells were collected, fixed at room temperature with 2.5% glutaraldehyde overnight at 4°C and dehydrated with a series of graded alcohols after 1% tetroxobin fixation for 1–2 hours. The samples were embedded in epoxy resin and observed via CM-120 transmission electron microscopy (Philips, the Netherlands).

Western Blot Analysis

RIPA buffer containing 1mmol/L PMSF was used to extract total protein from treated cells and tissues, and a BCA protein assay kit was used to determine the protein concentration. Protein bands were detected via SDS-PAGE and then transferred to a polyvinylidene difluoride membrane. The proteins were closed with sealing fluid and washed with phosphate-buffered saline and Tween three times for 15 minutes each time. The PVDF membrane was incubated with primary antibody at 4°C overnight. After three washes, the membrane was incubated with secondary antibody at room temperature for 1 hour, and actin was used as the control. Finally, the membrane was laid flat on a tray, chromogenic liquid was evenly added with a liquid transfer gun, and the membrane was exposed using a GE chemiluminescence imager (General Electric, USA). The Western blotting grayscale was determined using Image J software.

The primary antibody information was as follows: anti-PCNA (SC-71858, Santa, USA), anti-CDK2 (18048S, CST, USA), anti-CDK4 (12790S, CST, USA), anti-γH2AX (7631S, CST, USA), anti-LC3BI/II (ab51520, Abcam, USA), anti-ATG7 (ab53255, Abcam, USA), anti-p62 (ab56416, Abcam, USA), anti-Beclin1 (ab210498, Abcam, USA), anti-mTOR (2972S, CST, USA), anti-p-mTOR (2971S, CST, USA), anti-Akt (9272S, CST, USA), anti-p-Akt (13038S, CST, USA), and anti-β-actin (3700S, CST, USA).

Patient-Derived Organoids

Patient Samples

Tumor samples were from one patient with HGSOC and one patient with ENOC at Renji Hospital for short-term organoid generation and subsequent experiment. Written informed consent was obtained for all subjects and the study was approved by Shanghai Jiao Tong University School of Medicine, Renji Hospital Ethics Committee (Ethic number KY2020-114). This was conducted in accordance with the Declaration of Helsinki.

Organoid Establishment and Culture

Tumor specimens were acquired immediately during the surgery preserving in DMEM serum-free medium and transported to the laboratory on ice within 2 hours. On arrival, tissue was minced, washed with PBS, digested with tumor dissociation kit. The digested tissue

Table 2 IC50 of STC and Cisplatin in HGSOC105 and ENOC107 at 5d

IC50 of STC and Cisplatin in HGSOC105 and ENOC107 at 5d (μM)		
	STC	**Cisplatin**
HGSOC105	0.2889	7.573
ENOC107	0.3547	1.759

suspension was strained over a 100-μm filter, centrifuged at 1500 rpm for 5 minutes, the pellet was resuspended in 5 mL PBS. In case of a visible red pellet, erythrocytes were lysed in 2 mL red blood cell lysis buffer for 5 minutes at room temperature followed by an additional wash with PBS and centrifugation at 1500 rpm. Cells were mixed with growth factor reduced Matrigel, with the final concentration of Matrigel at 50%, and the suspension was then rapidly plated into a 6-well plate. Once the Matrigel was solidified, 1mL of complete culture medium was added to each well. The composition of the complete medium was referred to the protocol provide by Kopper et al.[24] PDOs were kept in a humidified atmosphere of 5% CO_2 and 95% air at 37°C, and medium was changed every 5–7 days.

Organoid Viability Assay

Organoids were released from the Matrigel by incubating in Gentle Cell Dissociation Reagent for 30 minutes at room temperature. After counting, the organoids were suspended with Matrigel (200–500/μL) and seeded in a 96-well plate at 20 μL per well. When the Matrigel was solidified, 80 μL of complete culture medium was added to each well. Drugs were added 4 days after embedding. Cell viability was assayed using CellTiter-Lumi™ on day 5. Data analyses were performed using the GraphPad Prism software version 9.0 to calculate IC50 (Table 2).

Tumor Xenograft Assay

Nude mice (female, 4 weeks old) were purchased from Shanghai Super B&K Laboratory Animal Corp. (Shanghai, China) and used for the in vivo study according to the regulations of the Animal Protection and Utilization Committee of Shanghai University of Traditional Chinese Medicine (Ethic number P2SHUTCM200904006). A2780 were collected with PBS, and cells suspension was subcutaneously injected at a concentration of 2×10^7 cells/mL (100 μL). As the tumor grew to approximately 100 mm3, the mice were randomly divided into three groups: the control group (saline, i.p.), STC group (0.5 mg/kg i.p.) and Cisplatin group (2 mg/kg i.p.) (n=7). Saline, STC and cisplatin were injected every 2 days for 15 days. Tumor volume and mouse weight were measured every 2 days. Calipers were used to obtain tumor length (L) and width (W), and the following formula was used to calculate tumor volume L × (W^2)/2.

Immunohistochemistry and H&E Staining

Tumor tissue samples isolated from nude mouse were subjected to histological analysis. The tissues were immediately fixed in 4% paraformaldehyde for 24 hours and embedded in paraffin. The embedded sections were sliced into 5μm sections for immunohistochemical (IHC) staining. The tumors and mouse major organs were stained with H&E after being cut into 4μm sections, and histological examination was performed with an Olympus microscope.

Statistical Analysis

Experimental data were analyzed using GraphPad Prism software version 9.0. The results are representative of at least three independent experiments and are shown as mean ± standard error of the mean. *p<0.05, **p < 0.01, and ***p < 0.001 were considered statistically significant.

Results

STC Repressed Ovarian Cancer Cell Proliferation

To evaluate the anti-proliferative effects of STC on human ovarian cancer, two human ovarian cancer cell lines A2780 and SKOV3 were exposed to various concentrations of STC for 24 and 48 hours. The CCK-8 assay results showed that STC significantly inhibited the growth of these OC cell lines in a dose- and time-dependent manner (Figure 1A, Table 1). Consistent with the relative effects on cell viability, Western blotting results showed that STC reduced the expression of PCNA protein as the pharmacodynamic marker of proliferation in a dose-dependent manner (Figure 1B). Moreover, at concentration of 0.5 μM and 1 μM, STC significantly reduced the colony formation of A2780 and SKOV3 cells (Figure 1C). Thus, the potential anti-proliferative effect of STC was indicated in ovarian cancer cells.

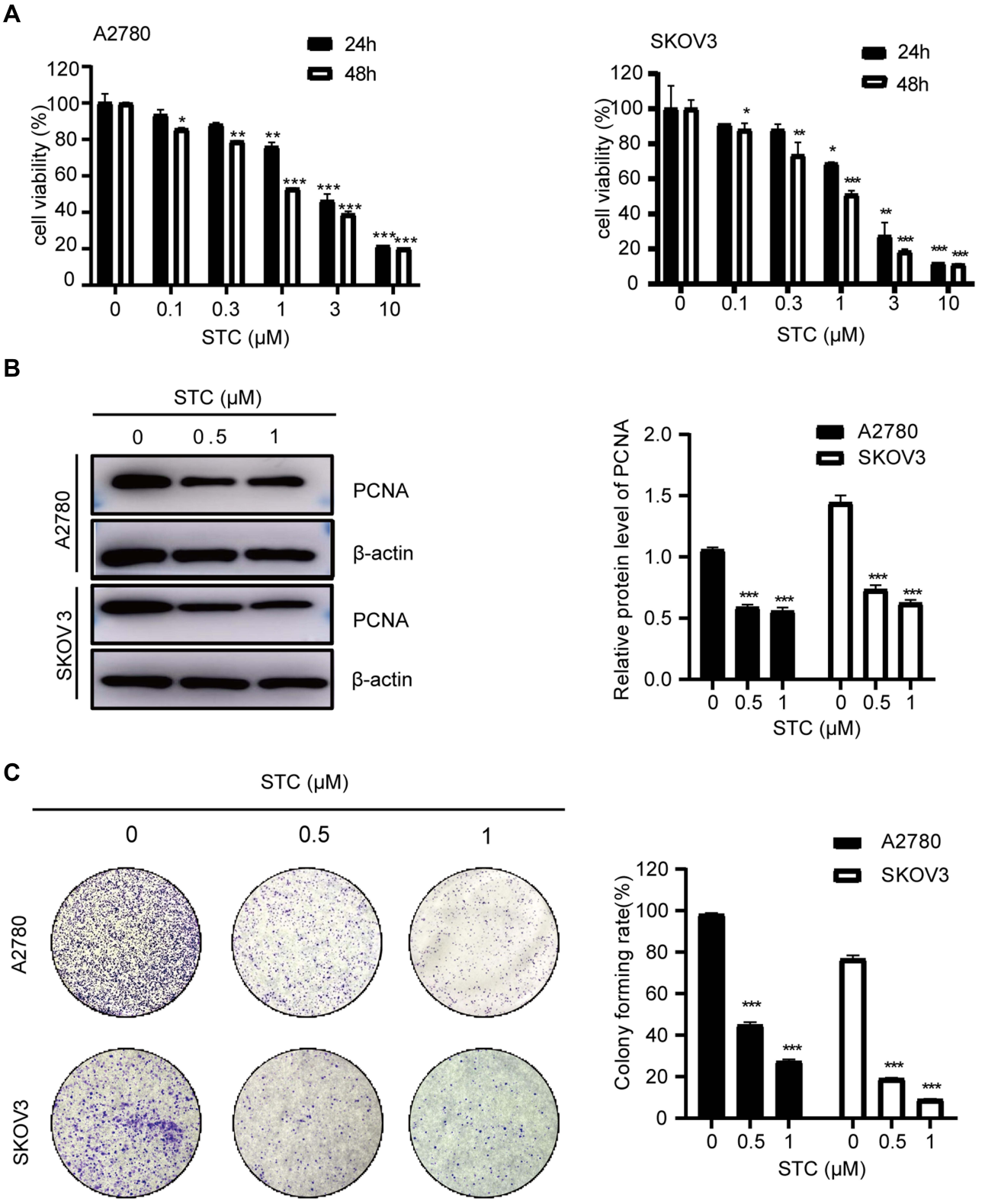

Figure 1 STC repressed ovarian cancer cell proliferation. (A) Two human ovarian cancer cell lines A2780 and SKOV3 cells were untreated or treated with different concentrations (0–10 μM) of STC for 24 and 48 hours, and the cell viability was measured by CCK-8 assay. (B) A2780 and SKOV3 cells were treated with STC at 0, 0.5 and 1μM for 48 hours, and the proliferation-related protein PCNA detected by Western blotting. (C) STC inhibited the colony formation ability of A2780 and SKOV3 cells. Data are presented as the mean ± SEM of three independent experiments, *P <0 0.05, **P <0.01, ***P<0 0.001, n=3.

https://doi.org/10.2147/OTT.S340556 DovePress

STC Induced Cell Cycle Arrest and Promoted Apoptosis in Ovarian Cancer Cells

To further explore whether STC-induced growth inhibition was associated with cell cycle regulation, we assessed the cell cycle distribution by flow cytometry subsequently. Compared with control cells, STC treatment for 48 hours mainly induced cell cycle arrest at the G0/G1 phase and led to the corresponding decrease in S and G2/M phase in both A2780 and SKOV3 cells (Figure 2A). Then, we used Western blotting to detect cyclins and cyclin-dependent kinases (CDKs) in different phases and checkpoint response after STC treatment for 48 hours. In both OC cell lines, STC showed a dose-dependent inhibition of the CDK2 and CDK4 expression, which are known to be involved in G1/S checkpoint (Figure 2B).

It was established that DNA damage could cause cell phase arrest and result in DNA damage repair response. As a typical indicator of DNA damage, the level of γ-H2AX was examined in both STC-treated OC cells. The results suggested that the expression of γ-H2AX was significantly increased after treatment of STC for 48 hours (Figure 2C). When DNA damage is beyond the capacity of DNA repair, it eventually led to cell apoptosis.[25] Consequently, STC significantly induced cell apoptosis or cell necrosis in the two cells after 48 hours treatment, as evidenced by Annexin V-FITC/PI double staining by flow cytometric

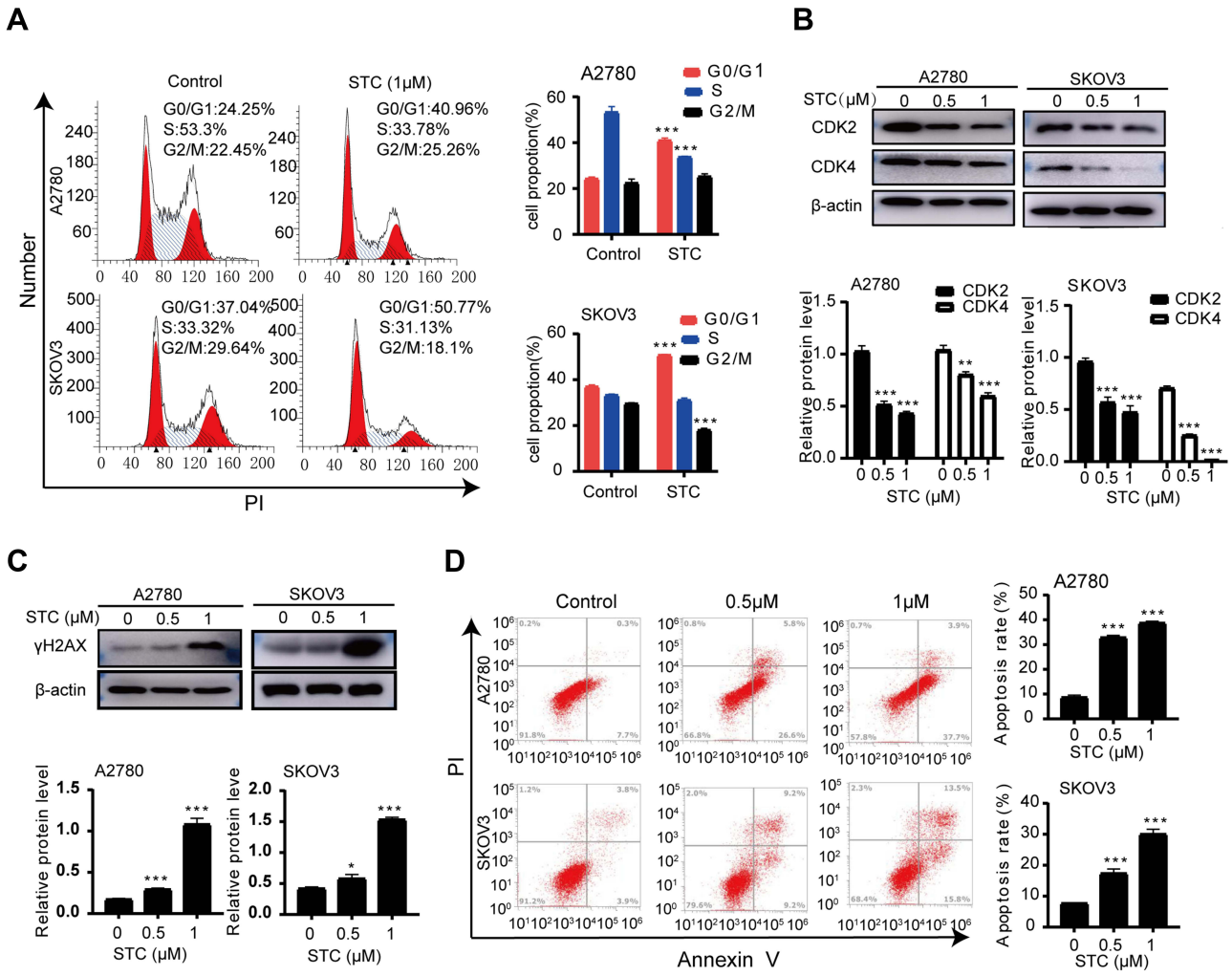

Figure 2 STC induced cell cycle arrest and promoted apoptosis in ovarian cancer cells. (**A**) Cell cycle distributions of A2780 and SKOV3 treated with STC for 48 hours were detected by flow cytometric assay. (**B**) A2780 and SKOV3 cells were treated with various concentrations (0, 0.5 and 1μM) for 48 hours, and the expression of CDK2 and CDK4 were compared by Western blot analysis. (**C**) A2780 and SKOV3 cells were treated with STC at 0, 0.5 and 1μM for 48 hours, and the expression of γH2AX were compared by Western blot analysis. (**D**) A2780 and SKOV3 cells were treated with STC at 0, 0.5 and 1μM for 48 hours, and then apoptotic cells were detected with the Annexin V-PI kit and analyzed by flow cytometry. Data are presented as the mean ± SEM of three independent experiments, *P <0.05, **P <0.01, ***P <0.001, n=3.

analysis (Figure 2D). Collectively, these data suggest that STC could result in severe DNA damage and induce cell cycle arrest and apoptosis in OC cells.

STC Induced Autophagy in Ovarian Cancer Cells

Since autophagy has been demonstrated as a tumor suppressor in some cancer types, we next investigate whether STC induced autophagy in OC cell lines. Accumulating evidence has revealed that LC3-II is an important autophagosome marker, and p62 is a selective autophagy receptor that is degraded within the autolysosome after an increase in autophagic flux.[26] After STC treatment, the ratio of LC3-II/ I was elevated and the level of p62 was decreased in a dose-dependent manner in A2780 and SKOV3 cells as compared to control cells, which indicates that STC could promoted the turnover of LC3-II and p62 degradation (Figure 3A). Moreover, the key autophagy-related gene (ATG) encoding proteins including ATG7 and Beclin1 were also significantly upregulated after STC treatment (Figure 3A). To visualize LC3-labelled cytoplasmic vacuolation to further clarify whether the complete progression of autophagy was affected by STC, the mRFP-GFP-LC3 reporter was used to monitor and quantify autophagic flux inside cells. As shown in Figure 3B, A2780 and SKOV3 cells treated with STC (1 μmol/L) for 24 h had accumulated detectable yellow autophagic LC3 puncta (mRFP+/GFP+) inside the cytoplasm compared with untreated controls. Furthermore, we examined autophagosome formation after STC treatment via transmission electron microscopy (TEM). Two cells were treated with STC for 24 hours, and large numbers of autophagosomes (indicated by red arrows) were easily observed in treated cells (Figure 3C). Collectively, these results demonstrated that STC activated autophagy in ovarian cancer cells.

Autophagy Inhibitors Enhanced STC-Induced Growth Inhibition and Apoptosis

To evaluate whether STC induced autophagy is related to cell proliferation and apoptosis, we used an autophagy inhibitor 3-MA to block the autophagy process. Western blot data showed the effect of STC on LC3-II and p62 accumulation was compromised in the presence of 3-MA. The regulations of autophagy-related proteins including Beclin1, ATG7 by STC were also impeded in the presence of 3-MA (Figure 4A). Moreover, confocal microscopy was used to analyze mRFP and GFP LC3 puncta. As shown in Figure 4B, 3-MA could significantly inhibit STC-induced autolysosome accumulation, consistent with the Western blot results. These results further demonstrated the role of STC in activating autophagy of OC cells, which could be partly rescued by 3-MA. In addition, we observed a synergistic inhibition on OC cell lines by STC and 3-MA. Interestingly, compared with STC treatment alone, CCK-8 assays showed that 3-MA combined with STC strengthened the inhibitory effect in A2780 and SKOV3 cell lines (Figure 5A). Similarly, according to the results of Annexin V/PI assays, the combination of STC with 3-MA also significantly increased the number of apoptotic ovarian cancer cells than STC treatment alone (Figure 5B). All these results demonstrated that autophagy inhibitor enhanced the antitumor effects of STC in ovarian cancer cells.

STC Induced Autophagy via Inhibiting the AKT/mTOR Signaling Pathway

The AKT/mTOR signaling pathway plays a crucial role in autophagy and apoptosis.[15,27] Thus, to ascertain whether the AKT/mTOR signaling pathway participates in STC-induced events in OC cells, we first evaluated the effects of STC on key proteins associated with the AKT/mTOR signaling pathway. The expression and phosphorylation levels of AKT and mTOR in STC-treated ovarian cancer cells were analyzed using a Western blot analysis. It was shown that STC treatment did not alter the expression of total AKT or mTOR but significantly reduced the phosphorylation level of AKT and mTOR in a dose-dependent manner (Figure 6A). To further investigate the role of AKT/mTOR signaling pathway in STC-induced autophagy, MK2206 (an AKT inhibitor) and rapamycin (an mTOR inhibitor) were used to inhibit the AKT/mTOR signaling pathway respectively. Our finding showed that STC combined with MK2206 had a more obvious inhibitory effect on p-AKT and p-mTOR and LC3B-II conversion was significantly increased than STC alone (Figure 6B). Moreover, Rapa significantly reduced p-mTOR expression and increased LC3B-II conversion in STC-treated cells (Figure 6C). Collectively, these findings illustrate that inhibition of the AKT/mTOR pathway is required for STC-induced autophagy in ovarian cancer cells.

Effects of STC on Patient-Derived Ovarian Cancer Organoids

PDO preserving tumor heterogeneity has been successfully applied to test and develop therapeutic approaches in preclinical settings.[28] In order to appreciate the effects of STC in

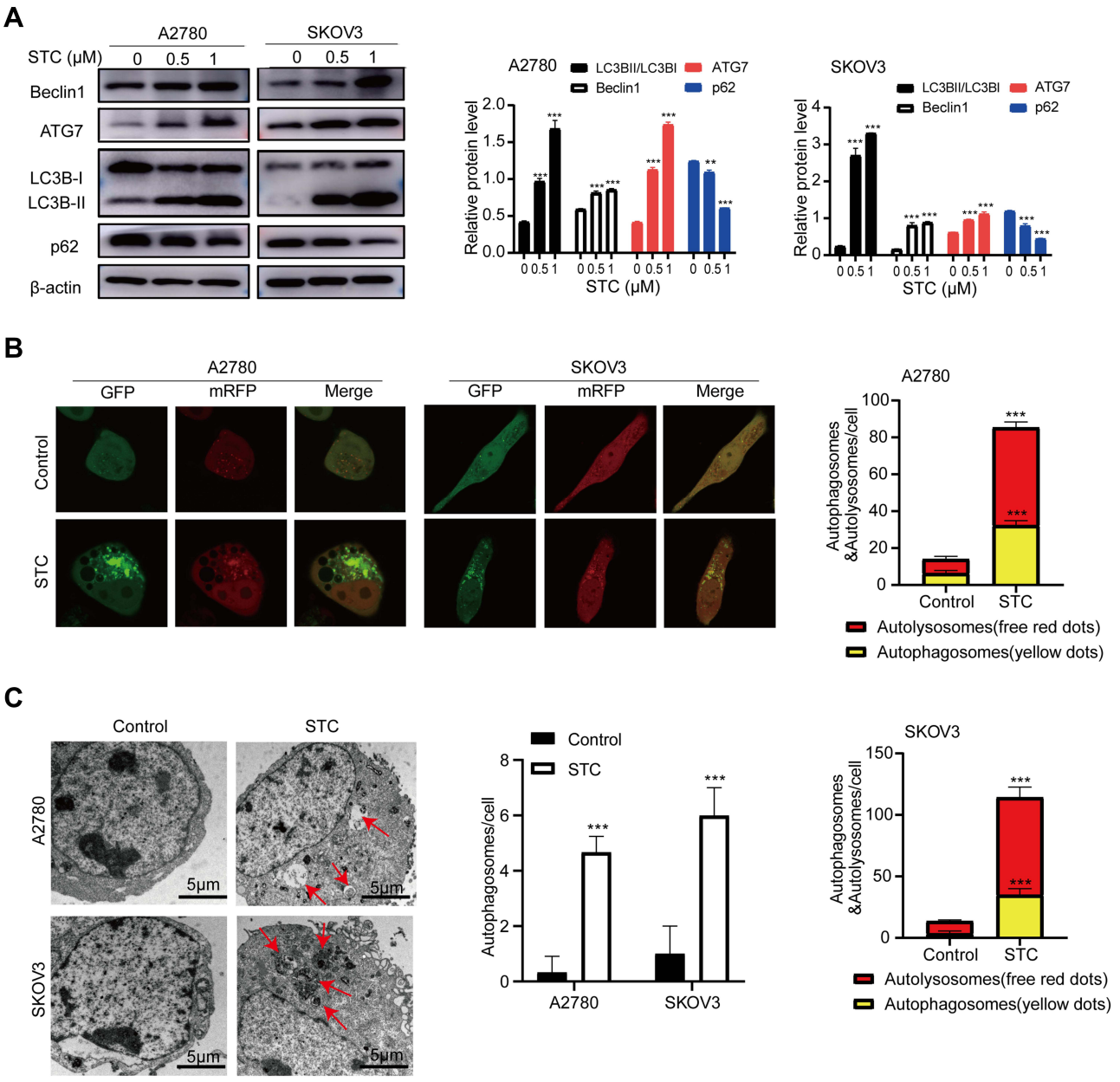

Figure 3 STC induced autophagy in ovarian cancer cells. (**A**) The expression of autophagy-associated protein (Beclin1 and ATG7) and autophagic substrates (LC3B and p62) were analyzed in A2780 and SKOV3 cells after STC treatment at 0, 0.5, and 1μM for 48 hours by Western blotting. (**B**) A2780 and SKOV3 cells overexpressing GFP-mRFP-LC3 were treated with STC (0 and 1μM) for 24 hours and then subjected to confocal microscopy. Scale bar: 10μm. (**C**) Ultrastructural features of A2780 and SKOV3 cells treated with STC (0 and 1μM) for 48 hours were analyzed by electron microscopy. Autophagosomes (Red arrows) are shown at high magnification. Scale bar: 5μm. The number of autophagosomes in A2780 and SKOV3 cells is presented. Data are presented as the mean ± SEM of three independent experiments, **P <0.01, ***P <0.001, n=3.

a model closer to clinical situation, we tested these treatments on ovarian cancer organoids (cisplatin as a positive control). Two organoid lines (HGSOC-105 and ENOC-107) were established from ovarian cancer patients, and the histology of organoids lines was confirmed. These organoids were treated with STC and cisplatin for 5 days, respectively. Consistent with the results of OC cell line-based assays, STC significantly repressed the viability of these two OC PDOs and IC50 values were both lower than 1 μM (Figure 7A, Table 2). Moreover, the therapeutic effect of STC was better than that of cisplatin, suggesting its potential clinical efficacy (Figure 7A and B).

STC Exhibited Antitumor Efficacy in OC Subcutaneous Xenograft Models

To evaluate the pharmacological effect of STC in vivo, we generated subcutaneous A2780 xenograft models. Compared

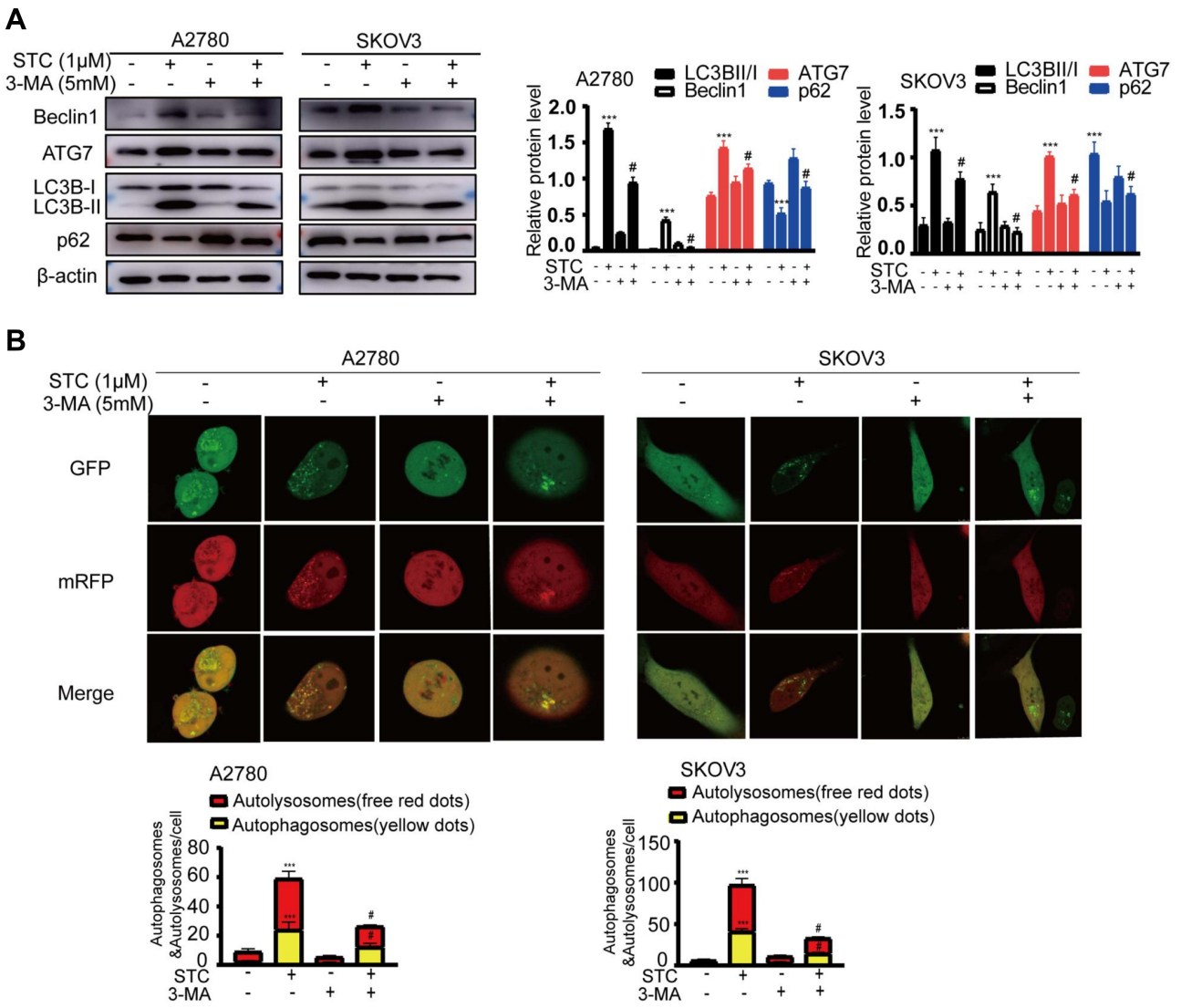

Figure 4 STC-induced autophagy could be inhibited by autophagy inhibitors. (**A**) The expression of autophagy-associated proteins (Beclin1 and ATG7) and autophagic substrate (LC3B and p62) were analyzed by Western blotting in A2780 and SKOV3 cells after treatment with STC (1 μM), 3-MA (5 mM) or combination for 48 hours. (**B**) A2780 and SKOV3 cells overexpressing GFP-mRFP-LC3 were treated with STC (1μM), 3-MA (5 mM) or combination for 24 hours and then subjected to confocal microscopy. Scale bar: 10μm. Data are presented as the mean ± SEM of three independent experiments, #P<0.05, ***P <0.001, n=3.

with the control group, the growth of xenograft tumors was strongly inhibited by STC treatment, and the volume and weight of tumors were significantly decreased, while there was no significant effect on the body weight of the mice ($p<0.05$) (Figure 8A–D). Western blotting was used to validate the expression of LC3B, p62, PCNA and γH2AX. The data were consistent with the cell experiments in vitro (Figure 8E). H&E staining showed that there were many areas of necrosis in tumor tissues of the STC-treated group (Figure 8F). Moreover, IHC staining provided additional evidence that OC tumor regression was associated with decreased proliferation (PCNA), increased γH2AX and LC3BI/II levels in xenografts after treatment with STC (Figure 8F). These data showed that STC could inhibit tumor growth by activating apoptosis and inducing autophagy in vivo. Finally, the results of H&E pathological sections of mice major organs (heart, liver, spleen, lung and kidney) indicated that STC treatment had no evident damage to the major organs of mice (Figure 8G).

Discussion

Natural products have been considered as an important source of new drug discoveries and are of great value to medicine. STC was isolated from the sea cucumber Thelenota anax by our lab, and previous studies have shown that STC negatively regulates cell proliferation by inducing apoptosis in leukemic

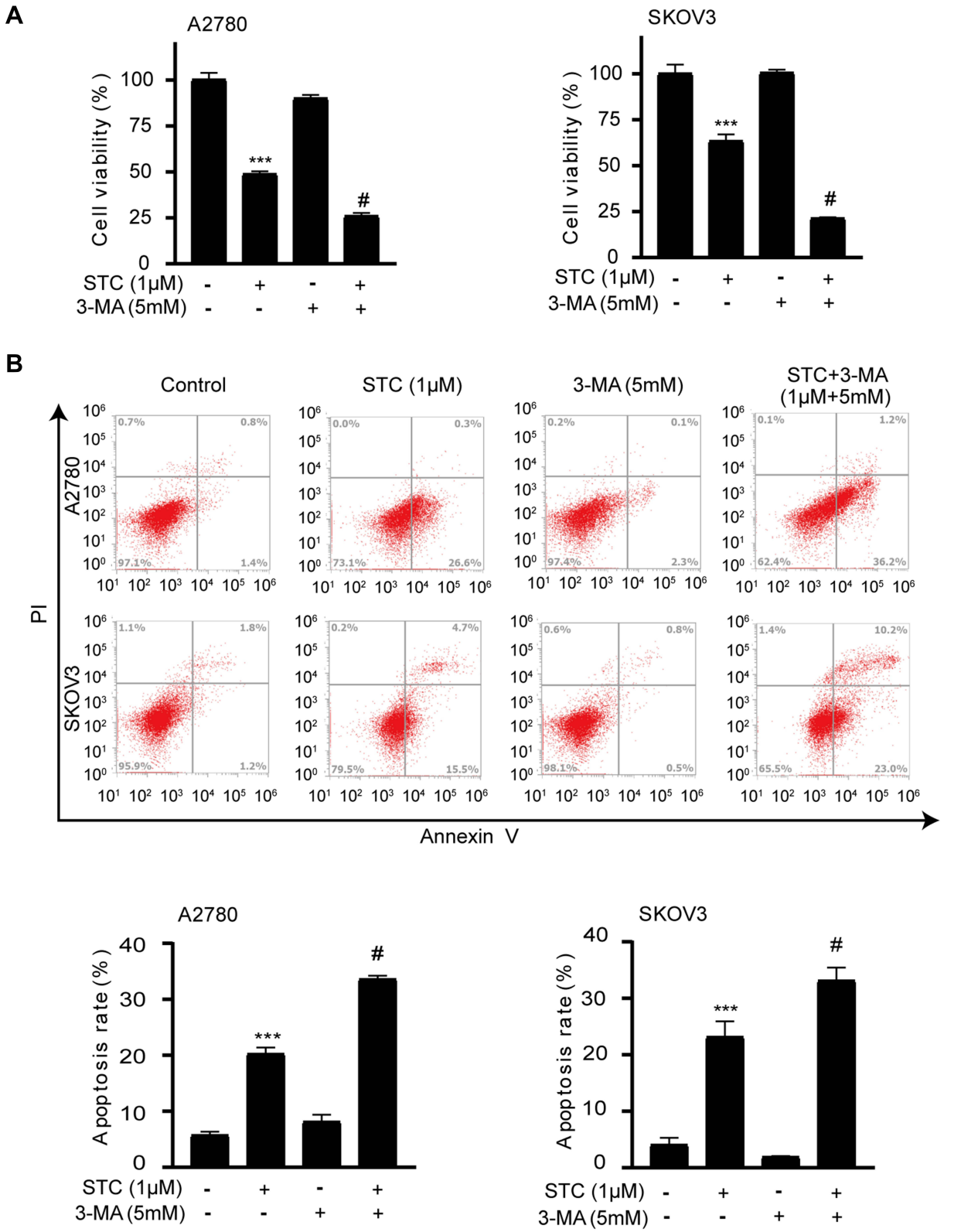

Figure 5 Autophagy inhibitors enhanced STC-induced apoptosis and growth inhibition. (**A**) CCK-8 assays of A2780 and SKOV3 cells after STC treatment with STC (1 μM), 3-MA (5 mM) or 3-MA plus STC (5 mM+1 μM) for 48 hours. (**B**) Apoptosis assays of A2780 and SKOV3 cells after STC treatment with STC (1 μM), 3-MA (5 mM) or 3-MA plus STC (5 mM+1 μM) for 48 hours by flow cytometry. Data are presented as the mean ± SEM of three independent experiments, compare to STC, ***P <0.001; compared to 3-MA plus STC, #P <0.05, n=3.

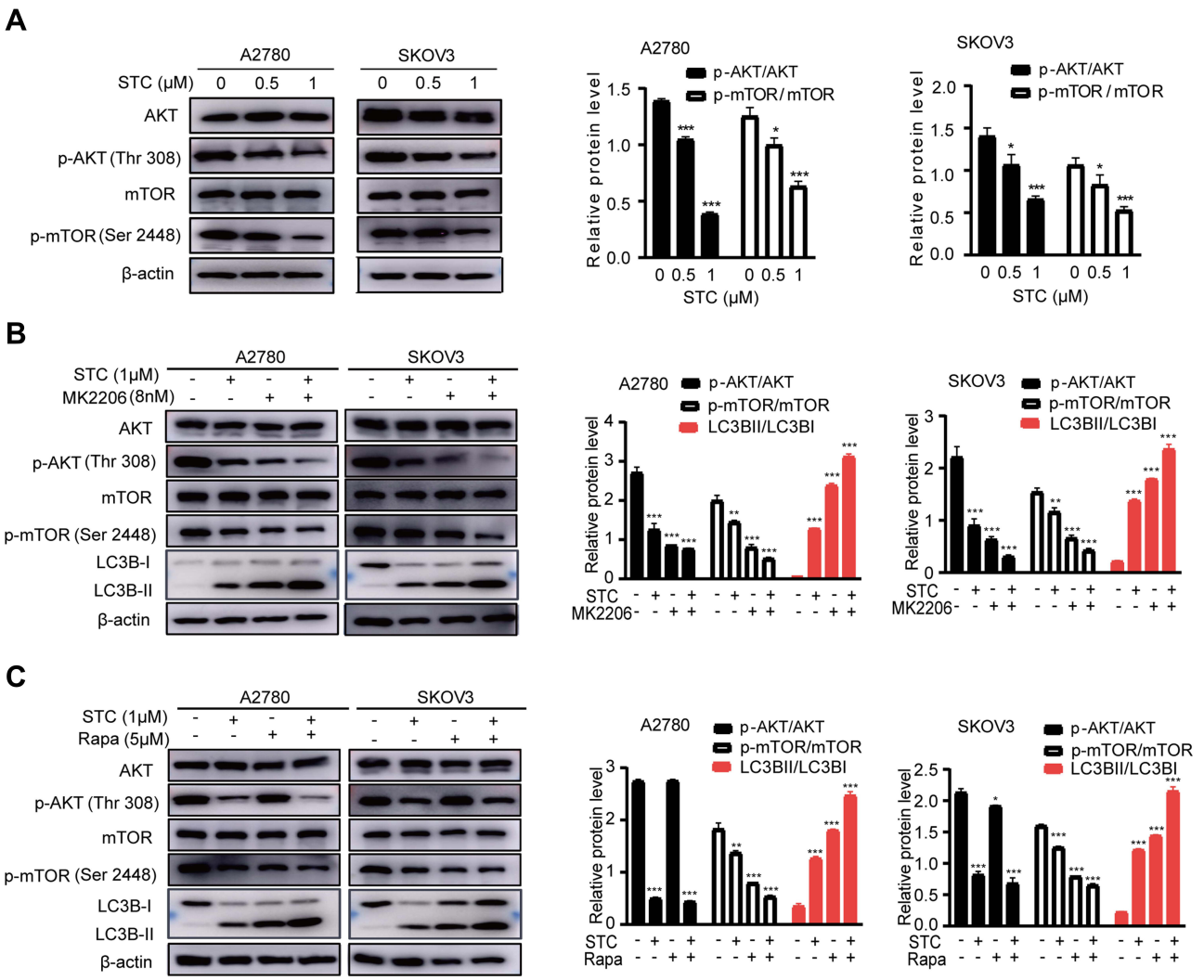

Figure 6 STC induced autophagy by inhibiting the AKT/mTOR signaling pathway. (**A**) The expression of AKT, p-AKT (Thr 308), mTOR and p-mTOR (Ser 2448) were analyzed by Western blotting in A2780 and SKOV3 cells after exposed to various concentrations of STC (0, 0.5, and 1 μM) for 48 hours. (**B**) A2780 and SKOV3 cells were treated with or without STC (1 μM) in combination with MK2206 (8 nM) for 48 hours. AKT, p-AKT (Thr 308), mTOR, p-mTOR (Ser 2448) and LC3B-II/I were detected by Western blotting. (**C**) A2780 and SKOV3 cells were treated with or without STC (1 μM) in combination with Rapa (5 μM) for 48 hours. AKT, p-AKT (Thr 308), mTOR, p-mTOR (Ser 2448) and LC3B-II/I were detected by Western blotting. Data are presented as the mean ± SEM of three independent experiments, *P <0.05, **P <0 0.01, ***P <0 0.001, n=3.

and colorectal cancer cells through the generation of ceramide.[13] We here for the first time revealed that STC displayed significant growth inhibition effects of ovarian cancer in vitro and in vivo by inducing autophagy through regulating the AKT/mTOR signaling pathway.

In the present study, two OC cell lines, A2780 and SKOV3, that are sensitive to STC treatment were chosen for functional studies, and they were characterized by reduced cell survival, cell cycle arrest and suppression of colony formation. These results demonstrated that STC treatment suppressed the malignant phenotype of OC. Induction of cell cycle arrest and apoptosis have become efficient strategies for cancer treatment.[29] STC also caused DNA damage and led to a decrease in the level of cell cycle regulatory molecules of G0/G1 checkpoint and induced apoptosis simultaneously in both human OC cells.

Growing evidence indicated that mechanisms regulating programmed cell death, including apoptosis, autophagic cell deaths and programmed necrosis.[30] However, the mechanisms by which process in cancer therapy is complex. During autophagy, autophagosomes engulf cytoplasmic components, including cytosolic proteins and organelles. Concomitantly, a cytosolic form of LC3 (LC3-I) is conjugated to phosphatidylethanolamine to form LC3-phosphatidylethanolamine conjugate (LC3-II), which is recruited to autophagosomal membranes.[31] In our study, the level of LC3-II was elevated

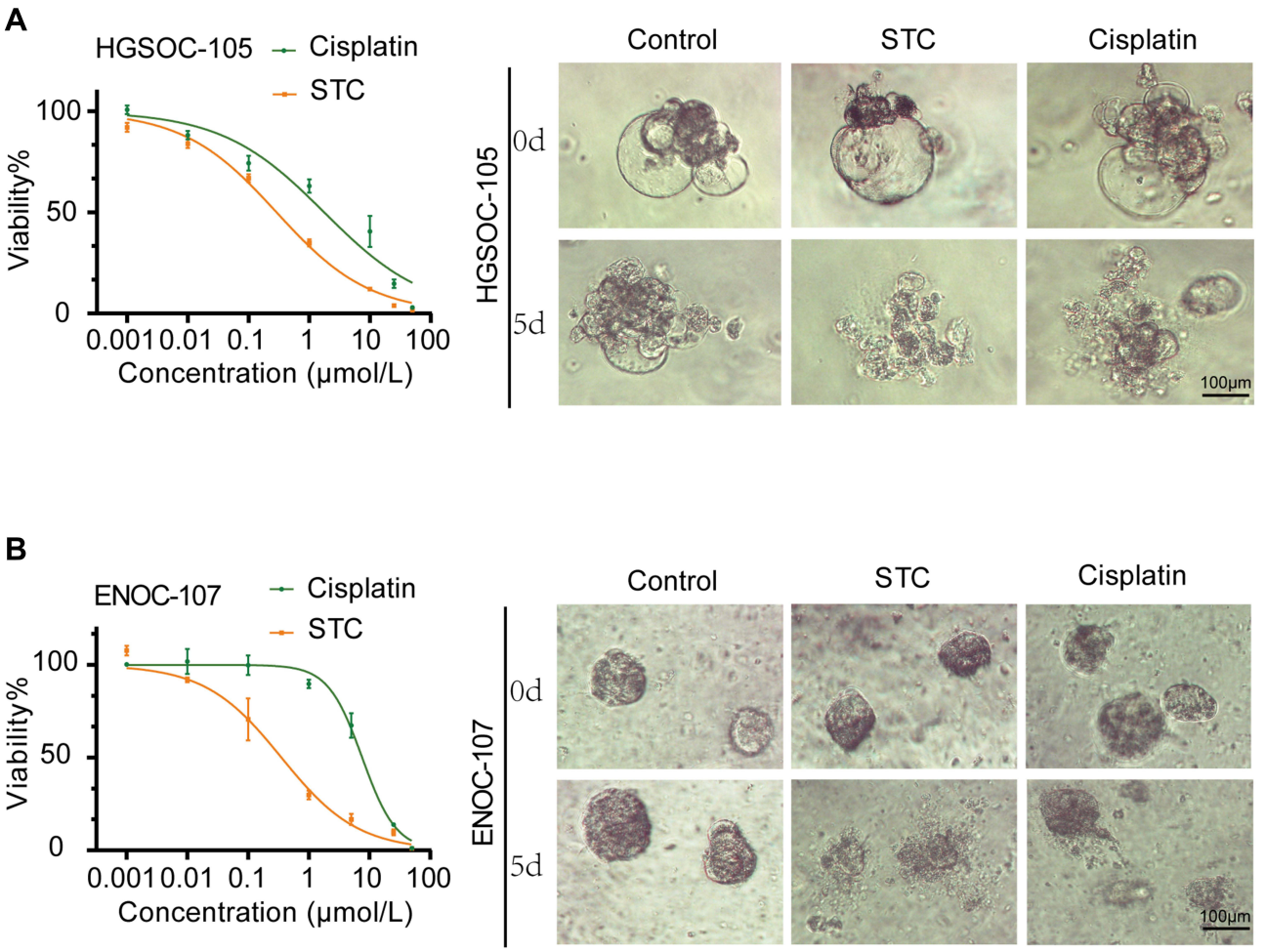

Figure 7 Effects of STC on patient-derived ovarian cancer organoids. (**A**) Two OC PDOs (HGSOC-105 and ENOC-107) were treated with various concentrations of STC and cisplatin (0, 0.001, 0.01, 0.1, 1, 10, 100 μM) for 5 days. The cell viability was measured by CellTiter-Lumi™. (**B**) Representative photomicrographs of two OC PDOs treated with or without STC and cisplatin. Scale bar = 100 μm. Data were expressed as mean ± SEM of three independent experiments.

in STC-treated OC cells. However, the increased expression of LC3-II may also be a consequence of disrupted autophagic flux, autophagy initiation and/or impairment of the degradation capacity. Previous studies have shown that p62 negatively correlated with selective autophagic degradation, which could be degraded within the autolysosome through direct binding to LC3-II.[32] Thus, then we found that p62 levels was decreased upon STC treatment, implying an increase in autophagic flux. Confirmation of increased autophagic flux was also obtained by the mRFP-GFP-LC3 reporter protein. The ultrastructural morphological observations showed that the accumulation of autophagosomes increased. Furthermore, the ATG coded proteins are involved in autophagosome formation and consist of functional units.[33] Hence, we determined at which step the autophagosome formation is increased and found that key autophagy-related proteins including ATG7 and Beclin1 were significantly upregulated after STC treatment. Therefore, STC was able to promote the formation of autophagosomes rather than inhibit the formation of autolysosomes and promote autophagic flux.

In recent years, the role of autophagy in cancer therapy has attracted great attention. It is well known that the crosstalk between the processes of apoptosis and autophagy is very important to maintain the balance of the intracellular environment. Autophagy can act as a protective factor to inhibit apoptosis by promoting cell survival, autophagy can also result in increased apoptotic cell death. For example, some novel anticancer agents such as tigecycline induced autophagic cell death,[34] while other drugs, such as salinomycin and quercetin,[35,36] mediated protective autophagy to resist cell death. Further functional analysis demonstrated that 3-MA mediated autophagy inhibition significantly improved STC-induced apoptotic cell death, suggesting that STC induced autophagy plays a protective role in OC cells.

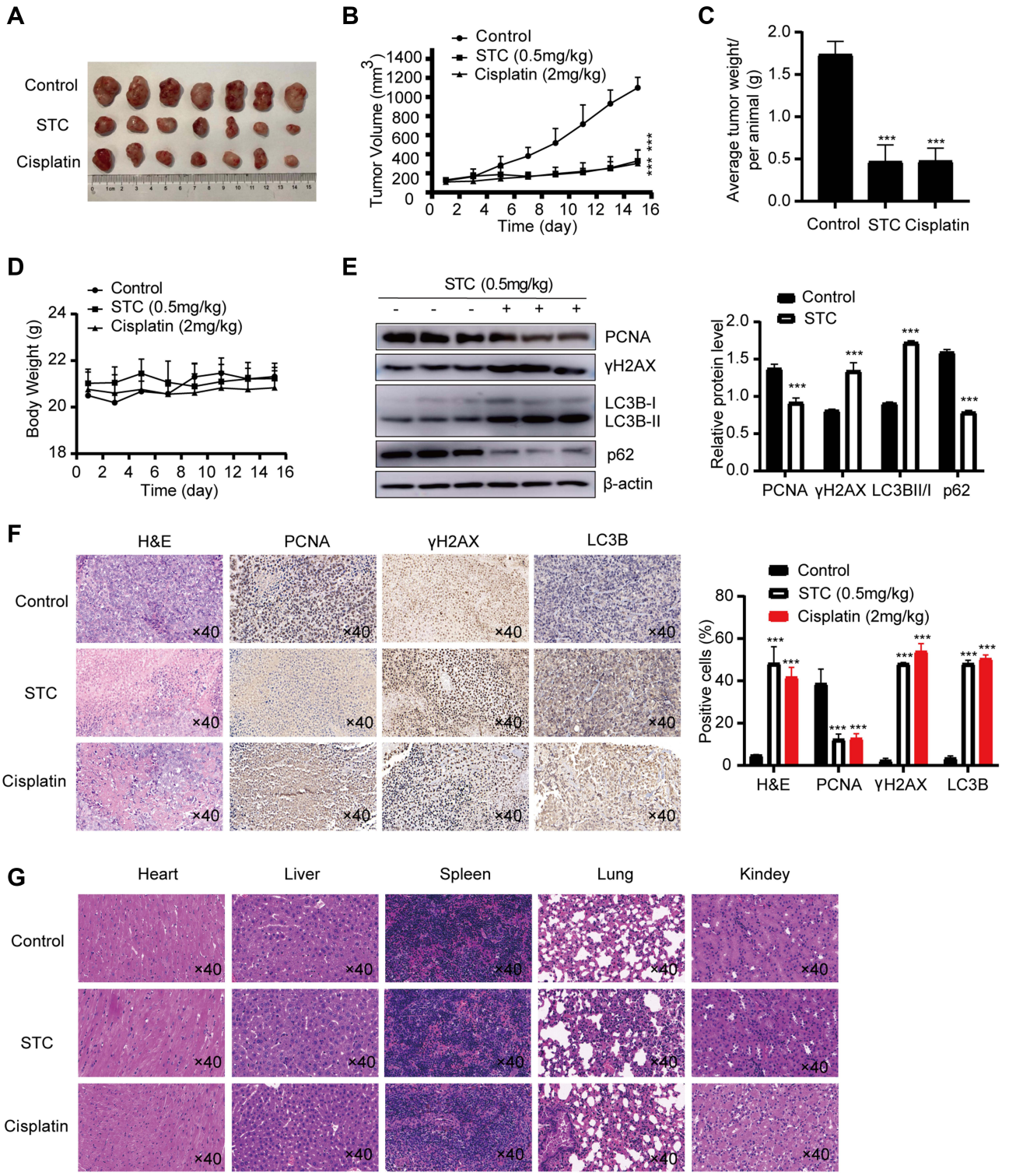

Figure 8 STC exhibited antitumor efficacy in OC subcutaneous xenograft models. (**A**) Representative images of subcutaneous tumors after treatment with STC (0.5mg/kg) or cisplatin (2mg/kg) (n = 7). (**B**) The volume and (**C**) weight of tumors was calculated in control, STC and Cisplatin group. Tumor volumes was calculated at different time points. (**D**) Body weight–time curve in control, STC and Cisplatin group. (**E**) The expression of PCNA, γH2AX, LC3B I/II and p62 in control and STC group were detected by Western blotting. (**F**) PCNA, γH2AX, LC3B I/II in STC and cisplatin group tumor tissues compared with the control group were detected by IHC staining. Original magnification: ×40. (**G**) Histopathology of the important organs. Original magnification: ×40. Data are presented as the mean ± SEM (n=7), ***P <0.001, n=3.

AKT and mTOR are both key regulators for autophagy.[35,37] As one of the most important intracellular signaling pathway, AKT/mTOR affects the status of downstream effector molecules through multiple pathways, autophagy activity can be negatively regulated by mediating the phosphorylation of mTOR.[38] Therefore, targeting AKT/mTOR-mediated autophagy is an important therapeutic strategy for a variety of tumors, and plays important roles in enhancing the chemosensitivity of tumor cells and avoiding drug resistance. Mounting evidence has suggested that numerous natural products are targeting AKT/mTOR-mediated autophagy, thereby suppressing tumor growth.[39,40] Thus, it was assumed that the AKT/mTOR signaling pathway may be involved in autophagy activated by STC in ovarian cancer cells. Our current data show that STC triggered the inhibition of AKT/mTOR, consistent with our hypothesis. Moreover, MK2206 (an AKT inhibitor) increased LC3-II conversion levels in STC-treated cells. In addition, the combination of rapamycin (an mTOR inhibitor) and STC in ovarian cancer cells also showed a similar synergistic effect. Collectively, these findings strongly support the hypothesis that suppression of the AKT/mTOR signaling pathway is involved in STC triggered protective autophagy.

To support and verify whether STC has the same capacity to suppress the growth of ovarian cancer in vivo, we examined the role of STC in xenograft nude mice. Using STC and cisplatin (as a positive control) in xenograft models to treat tumor-bearing mice, we found that STC had a significant inhibitory effect on tumor growth. Western blotting and IHC results revealed that STC induced apoptosis and autophagy in vivo, which are consistent with in vitro experimental results. In addition, it was shown that the apoptosis-promoting activity of STC was comparable to that of cisplatin, which further confirmed the effective antitumor effect of STC against ovarian cancer. Importantly, STC treatment did not show any abnormality in behavior or significant major organ-related toxicity, which is often had by cisplatin, such as nephrotoxicity, hepatotoxicity, cardiotoxicity. Regretfully, there are certain limitations in animal experiment owing to a single dose, and further studies in ovarian cancer animal models are necessary.

In summary, our study discovered a potential antitumor agent, STC, which exhibited strong antiproliferative efficacy in OC cell-based assays (OC cell lines and PDOs) and subcutaneous xenograft models. STC activated cytoprotective autophagy by inhibiting the AKT/mTOR pathway in ovarian cancer cells and combination therapy with an autophagy inhibitor showed significant synergetic effects on inhibiting proliferation and promoting apoptosis in vitro. The above inspiring results firstly provide pharmacological evidence for the future preclinical application of STC as a promising lead compound, alone or combined with autophagy inhibitors for human ovarian cancer treatment.

Acknowledgments

We would like to thank all the teachers in the Traditional Chinese Medicine Department and Research Center for Marine Drugs, State Key Laboratory of Oncogenes and Related Genes, Department of Pharmacy, RenJi Hospital, School of Medicine, Shanghai JiaoTong University, for their technical support. This study was supported by National Natural Science Foundation of China (Nos. 22137006, 82073713, U2106227, 81874479 and 82174135).

Disclosure

The authors report no conflicts of interest in this work.

References

1. Kuroki L, Guntupalli SR. Treatment of epithelial ovarian cancer. *BMJ*. 2020;m3773. doi:10.1136/bmj.m3773
2. Lheureux S, Braunstein M, Oza AM. Epithelial ovarian cancer: evolution of management in the era of precision medicine. *CA Cancer J Clin*. 2019;69(4):280–304. doi:10.3322/caac.21559
3. Ledermann JA. Front-line therapy of advanced ovarian cancer: new approaches. *Ann Oncol*. 2017;28:viii46–viii50. doi:10.1093/annonc/mdx452
4. Mirza MR, Coleman RL, González-Martín A, et al. The forefront of ovarian cancer therapy: update on PARP inhibitors. *Ann Oncol*. 2020;31(9):1148–1159. doi:10.1016/j.annonc.2020.06.004
5. Kurnit KC, Avila M, Hinchcliff EM, Coleman RL, Westin SN. PARP inhibition in the ovarian cancer patient: current approvals and future directions. *Pharmacol Ther*. 2020;213:107588. doi:10.1016/j.pharmthera.2020.107588
6. Correia-da-silva M, Sousa E, Pinto MMM, Kijjoa A. Anticancer and cancer preventive compounds from edible marine organisms. *Semin Cancer Biol*. 2017;46:55–64. doi:10.1016/j.semcancer.2017.03.011
7. Pangestuti R, Arifin Z. Medicinal and health benefit effects of functional sea cucumbers. *J Tradit Complement Med*. 2018;8(3):341–351. doi:10.1016/j.jtcme.2017.06.007
8. Aminin DL, Menchinskaya ES, Pisliagin E, et al. Anticancer activity of sea cucumber triterpene glycosides. *Mar Drugs*. 2015;13(3):1202–1223. doi:10.3390/md13031202
9. Dong J, Liang W, Wang T, et al. Saponins regulate intestinal inflammation in colon cancer and IBD. *Pharmacol Res*. 2019;144:66–72. doi:10.1016/j.phrs.2019.04.010
10. Shimada S. Antifungal steroid glycoside from sea cucumber. *Science*. 1969;163(3874):1462. doi:10.1126/science.163.3874.1462
11. Wargasetia TL, Permana S, Widodo N. Potential use of compounds from sea cucumbers as MDM2 and CXCR4 inhibitors to control cancer cell growth. *Exp Ther Med*. 2018. doi:10.3892/etm.2018.6588
12. Yoshida S, Shimada Y, Kondoh D, et al. Hemolytic C-type lectin CEL-III from sea cucumber expressed in transgenic mosquitoes impairs malaria parasite development. *PLoS Pathog*. 2007;3(12):e192. doi:10.1371/journal.ppat.0030192

13. Yun S-H, Park E-S, Shin S-W, et al. Stichoposide C induces apoptosis through the generation of ceramide in leukemia and colorectal cancer cells and shows in vivo antitumor activity. *Clin Cancer Res*. 2012;18(21):5934–5948. doi:10.1158/1078-0432.Ccr-12-0655
14. Granville CA, Memmott RM, Gills JJ, Dennis PA. Handicapping the race to develop inhibitors of the phosphoinositide 3-kinase/Akt/mammalian target of rapamycin pathway. *Clin Cancer Res*. 2006;12(3):679–689. doi:10.1158/1078-0432.Ccr-05-1654
15. Han W, Yu F, Cao J, et al. Valproic acid enhanced apoptosis by promoting autophagy via Akt/mTOR signaling in glioma. *Cell Transplant*. 2020;29:096368972098187. doi:10.1177/0963689720981878
16. Hong P, Liu Q-W, Xie Y, et al. Echinatin suppresses esophageal cancer tumor growth and invasion through inducing AKT/mTOR-dependent autophagy and apoptosis. *Cell Death Dis*. 2020;11(7). doi:10.1038/s41419-020-2730-7
17. LoPiccolo J, Blumenthal GM, Bernstein WB, Dennis PA. Targeting the PI3K/Akt/mTOR pathway: effective combinations and clinical considerations. *Drug Resist Updat*. 2008;11(1–2):32–50. doi:10.1016/j.drup.2007.11.003
18. Papadimitrakopoulou V, Adjei AA. The Akt/mTOR and mitogen-activated protein kinase pathways in lung cancer therapy.. *J Thorac Oncol*. 2006;1(7):749–751.
19. Gao L, Wang Z, Lu D, et al. Paeonol induces cytoprotective autophagy via blocking the Akt/mTOR pathway in ovarian cancer cells. *Cell Death Dis*. 2019;10(8). doi:10.1038/s41419-019-1849-x
20. Ediriweera MK, Tennekoon KH, Samarakoon SR. Role of the PI3K/AKT/mTOR signaling pathway in ovarian cancer: biological and therapeutic significance. *Semin Cancer Biol*. 2019;59:147–160. doi:10.1016/j.semcancer.2019.05.012
21. Popolo A, Pinto A, Daglia M, et al. Two likely targets for the anti-cancer effect of indole derivatives from cruciferous vegetables: PI3K/Akt/mTOR signalling pathway and the aryl hydrocarbon receptor. *Semin Cancer Biol*. 2017;46:132–137. doi:10.1016/j.semcancer.2017.06.002
22. Janku F, McConkey DJ, Hong DS, Kurzrock R. Autophagy as a target for anticancer therapy. *Nat Rev Clin Oncol*. 2011;8(9):528–539. doi:10.1038/nrclinonc.2011.71
23. Mizushima N, Levine B, Longo DL. Autophagy in human diseases. *N Engl J Med*. 2020;383(16):1564–1576. doi:10.1056/NEJMra2022774
24. Kopper O, de Witte CJ, Lõhmussaar K, et al. An organoid platform for ovarian cancer captures intra- and interpatient heterogeneity. *Nat Med*. 2019;25(5):838–849. doi:10.1038/s41591-019-0422-6
25. Gourley C, Balmaña J, Ledermann JA, et al. Moving from poly (ADP-ribose) polymerase inhibition to targeting DNA repair and DNA damage response in cancer therapy. *J Clin Oncol*. 2019;37(25):2257–2269. doi:10.1200/jco.18.02050
26. Mathew R, White E. Autophagy in tumorigenesis and energy metabolism: friend by day, foe by night. *Curr Opin Genet Dev*. 2011;21(1):113–119. doi:10.1016/j.gde.2010.12.008
27. Zhang X, Wang S, Wang H, et al. Circular RNA circNRIP1 acts as a microRNA-149-5p sponge to promote gastric cancer progression via the AKT1/mTOR pathway. *Mol Cancer*. 2019;18(1):1–24. doi:10.1186/s12943-018-0935-5
28. Driehuis E, Kretzschmar K, Clevers H. Establishment of patient-derived cancer organoids for drug-screening applications. *Nat Protoc*. 2020;15(10):3380–3409. doi:10.1038/s41596-020-0379-4
29. Schwartz GK, Shah MA. Targeting the cell cycle: a new approach to cancer therapy. *J Clin Oncol*. 2005. doi:10.1200/jco.2005.01.5594
30. Su Z, Yang Z, Xu Y, Chen Y, Yu Q. Apoptosis, autophagy, necroptosis, and cancer metastasis. *Mol Cancer*. 2015;14(1). doi:10.1186/s12943-015-0321-5
31. Tanida I, Ueno T, Kominami E. LC3 and autophagy. *Methods Mol Biol*. 2008. doi:10.1007/978-1-59745-157-4_4
32. Klionsky DJ, Abdalla FC, Abeliovich H, et al. Guidelines for the use and interpretation of assays for monitoring autophagy. *Autophagy*. 2012. doi:10.4161/auto.19496
33. Mizushima N, Yoshimori T, Ohsumi Y. The role of Atg proteins in autophagosome formation. *Annu Rev Cell Dev Biol*. 2011;27(1):107–132. doi:10.1146/annurev-cellbio-092910-154005
34. Tang C, Yang L, Jiang X, et al. Antibiotic drug tigecycline inhibited cell proliferation and induced autophagy in gastric cancer cells. *Biochem Biophys Res Commun*. 2014;446(1):105–112. doi:10.1016/j.bbrc.2014.02.043
35. Kim KY, Park KI, Kim SH, et al. Inhibition of autophagy promotes salinomycin-induced apoptosis via reactive oxygen species-mediated PI3K/AKT/mTOR and ERK/p38 MAPK-dependent signaling in human prostate cancer cells. *Int J Mol Sci*. 2017;18(5):1088. doi:10.3390/ijms18051088
36. Wang K, Liu R, Li J, et al. Quercetin induces protective autophagy in gastric cancer cells: involvement of Akt-mTOR- and hypoxia-induced factor 1α-mediated signaling. *Autophagy*. 2011;7(9):966–978. doi:10.4161/auto.7.9.15863
37. Xu Z, Han X, Ou D, et al. Targeting PI3K/AKT/mTOR-mediated autophagy for tumor therapy. *Appl Microbiol Biotechnol*. 2020. doi:10.1007/s00253-019-10257-8
38. Balakrishnan K, Peluso M, Fu M, et al. The phosphoinositide-3-kinase (PI3K)-delta and gamma inhibitor, IPI-145 (Duvelisib), overcomes signals from the PI3K/AKT/S6 pathway and promotes apoptosis in CLL. *Leukemia*. 2015;29(9):1811–1822. doi:10.1038/leu.2015.105
39. Rong L, Li Z, Leng X, et al. Salidroside induces apoptosis and protective autophagy in human gastric cancer AGS cells through the PI3K/Akt/mTOR pathway. *Biomed Pharmacother*. 2020;122:109726. doi:10.1016/j.biopha.2019.109726
40. Fan X-J, Wang Y, Wang L, Zhu M. Salidroside induces apoptosis and autophagy in human colorectal cancer cells through inhibition of PI3K/Akt/mTOR pathway. *Oncol Rep*. 2016;36(6):3559–3567. doi:10.3892/or.2016.5138